NANO LETTERS

ACS Editors' Choice

Letter

pubs.acs.org/NanoLett

Terms of Use

# Interface Control in Organic Electronics Using Mixed Monolayers of Carboranethiol Isomers

Jaemyung Kim,[†,∥] You Seung Rim,[‡,∥] Yongsheng Liu,[†,‡] Andrew C. Serino,[†,‡] John C. Thomas,[†,§] Huajun Chen,[‡] Yang Yang,*[,†,‡] and Paul S. Weiss*[,†,‡,§]

[†]California NanoSystems Institute, [‡]Department of Materials Science and Engineering, and [§]Department of Chemistry and Biochemistry, University of California, Los Angeles, Los Angeles, California 90095, United States

Supporting Information

**ABSTRACT:** We employ mixed self-assembled monolayers of carboranethiols to alter the work function of gold and silver systematically. We use isomers of symmetric carboranethiol cage molecules to vary molecular dipole moments and directions, which enable work function tunability over a wide range with minimal alterations in surface energy. Mixed monolayers of carboranethiol isomers provide an ideal platform for the study and fabrication of solution-processed organic field-effect transistors; improved device performance is demonstrated by interface engineering.

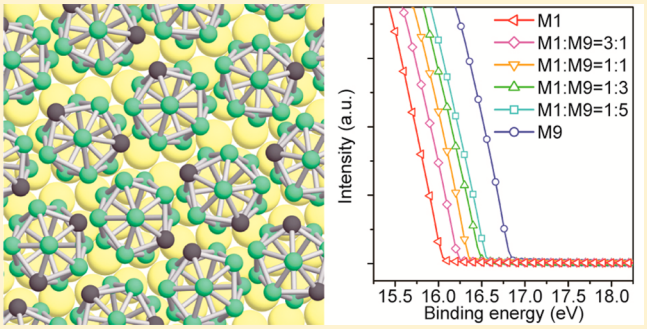


**KEYWORDS:** *Cage molecules, self-assembled monolayers, work function, surface energy, organic electronic devices, solution processing*

Recent advances in materials synthesis and interface engineering have produced significant improvements in the device performance of organic field-effect transistors (OFETs).[1−3] Solution-processed OFETs are of particular interest, as they can be manufactured at low temperatures on a large scale using cost-effective, high-throughput techniques.[4,5] Several factors collectively account for the device performance of solution-processed OFETs,[1,6] such as intrinsic electrical properties of organic semiconductors, processing conditions, the work function (WF) of source/drain (S/D) metal electrodes, and the interfacial properties between the S/D metal and the semiconductor. To facilitate efficient charge transport across the metal/semiconductor interface, the Fermi level of the metal electrode should align well with the highest occupied molecular orbital (HOMO) of p-type or the lowest unoccupied molecular orbital (LUMO) of n-type organic semiconductors, respectively.[7−10] This alignment can be achieved by selecting a metal with an appropriate WF[11−13] or by inserting an additional injection layer between the metal and the semiconductor.[14−16] For example, Zhou et al. have demonstrated that injection layers based on polymers containing aliphatic amine groups can reduce the WF of various conductors substantially, providing alternatives to chemically reactive low WF metals such as Ca or Mg.[17,18] Another approach is to place molecules with strong dipole moments at the metal/semiconductor interface by functionalizing the metal surface with self-assembled monolayers (SAMs),[19−27] whose formation is based on strong, self-limiting interactions between the metal, such as gold or silver, and thiol groups (−SH).[28] Changing the chemical composition of molecules used can alter the direction and the magnitude of surface dipole moments,[29,30] enabling the formation of energetically favorable metal/semiconductor interfaces.

A mixed SAM consisting of two or more thiol molecules with distinctly oriented dipole moments can aid in precise control over the interface WF.[31,32] Changing the surface coverage ratio of thiol molecules enables systematic alteration of the ensemble of local dipole moments, leading to near-continuous modulation of WF. However, one potential issue in using mixed SAMs in solution-processed OFETs is that the WF modulation usually involves the introduction of varying chemical functionality on the surface, which can significantly alter the surface properties. For example, fluorinated alkanethiols and unfunctionalized *n*-alkanethiols are the molecules most commonly used for this purpose either to increase or to decrease the metal WF, respectively.[19,21,22,29] By codepositing these two thiol molecules, precise modulation of the metal WF over a wide range has been demonstrated.[31] However, the introduction of $CF_3$ end groups in the mixed SAM dramatically alters the surface wettability and thus can induce significant differences in the thin film properties during subsequent deposition of solution-processed organic semiconducting layers, such as thickness, surface morphology, and even molecular ordering.[22,24,33,34] Flexible, linear alkanethiols produce a large number of various defects in SAMs, such as discrete lying down phases and tilt domain boundaries, adding another level of complexity to the interface.[35−37] As all of these factors can

**Received:** March 22, 2014
**Revised:** April 25, 2014
**Published:** April 28, 2014

   dx.doi.org/10.1021/nl501081q | *Nano Lett.* 2014, 14, 2946−2951

significantly affect the performance of OFETs, this variation adds further complications in the interpretation of the device characteristics. Moreover, the processing conditions need to be separately optimized for each surface condition to compensate for the thin film variations, complicating the device fabrication process. Therefore, to further our understanding of the device physics of solution-processed OFETs and to establish reliable processing conditions, it is highly desirable to develop robust interface systems in which the WF can be independently modulated without significantly changing surface properties.

Here, we demonstrate that mixed SAMs of carboranethiol isomers can be used to tune the WF of gold and silver continuously without causing significant variations in surface energy. Carboranethiol isomers (Figure 1a) have several

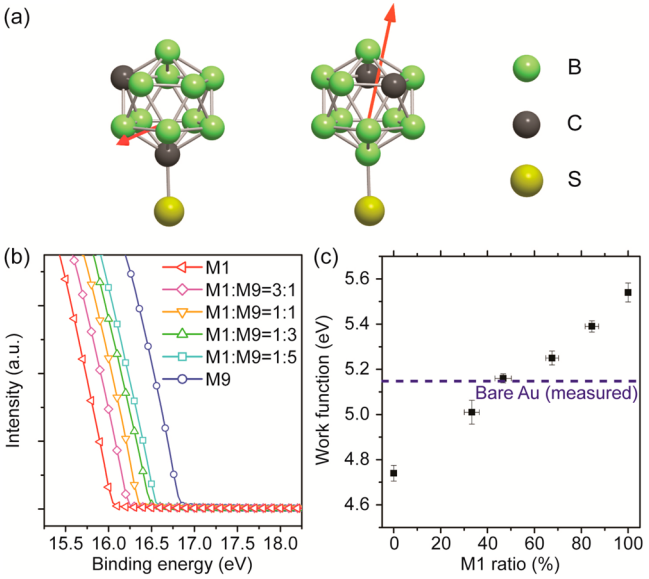


**Figure 1.** WF modulation of gold using mixed SAMs of carboranethiol isomers. (a) Chemical structures of carboranethiol isomers (**M1**, left; **M9**, right). Hydrogen atoms are omitted for clarity. Depending on the arrangement of atoms within the cage structure, the direction of dipole moment changes (arrows) while the chemical composition remains unchanged. (b) UPS spectra ($E_{SC}$ region) of the gold surfaces decorated with pure or mixed SAMs. The WF of gold can be systematically tuned by varying **M1**/**M9** ratios in deposition solutions. The surface coverage of each isomer can be estimated from PM-IRRAS spectra (Figure S1, Supporting Information). (c) As the surface coverage of **M1** increases, the WF of gold linearly increases from 4.74 eV (100% **M9**) to 5.54 eV (100% **M1**). The WF of bare gold was measured to be 5.15 eV (dashed line).

advantages over other thiol molecules, rendering them good candidates as WF modifiers. First, their molecular dipole moments can be systematically altered depending on the arrangement of atoms within the cage structure.[38−40] Therefore, stoichiometrically identical isomers can be used either to increase or to decrease the metal WF. Second, the number and types of defects within SAMs are greatly reduced by the symmetry of rigid and upright carboranethiols, leading to the formation of high-quality monolayers through simple processing.[39−42] Third, they have strong dipole moments within compact structures, and the molecules are stabilized by delocalized electrons.[43] Therefore, the tunneling resistance through the SAMs can be significantly lower than other SAMs. By employing mixed SAMs of carboranethiol isomers, we demonstrate that charge injection at the metal/semiconductor interface can be systematically modulated without causing variations in the organic thin film properties, and the device performance of solution-processed OFETs can be significantly enhanced.

Figure 1a shows carboranethiol isomers used in this work, namely *m*-carborane-1-thiol (**M1**, left) and *m*-carborane-9-thiol (**M9**, right), respectively. The two isomers were chosen as our model systems because (i) they have dipole moments strong enough to modify the metal WF (1.06 D for **M1**; 4.08 D for **M9**, calculated for gas-phase molecules);[39] (ii) they have substantially different dipole directions; and (iii) they are widely and commercially available. As the positive end of the dipole moment lies between the two carbon atoms, the **M1** dipole vector (pointing in the direction of positive charge) component normal to the surface points toward the thiol group, while that of **M9** points away from the thiol group (Figure 1a, arrows). Therefore, when they are deposited onto gold, **M1** and **M9** SAMs are expected to increase or to decrease the metal WF, respectively. This result was confirmed by ultraviolet photoelectron spectroscopy (UPS, Figure 1b). For the UPS measurements, carboranethiol SAMs were deposited on Au{111} substrates prepared by electron-beam evaporation (see Materials and Methods, Supporting Information). The WF ($\phi$) was determined by using the equation $\phi = h\nu - |E_{SC} - E_F|$, where $h\nu$ is the photon energy of the source (21.2 eV for He I), $E_F$ is the Fermi edge, and $E_{SC}$ is the secondary electron cutoff. As $E_F$ was fixed in all measurements, only $E_{SC}$ regions of the spectra are shown in Figure 1b. The WF of bare gold was measured to be 5.15 ± 0.02 eV (not shown). When the gold surface was decorated with the **M1** SAM, the $E_{SC}$ of the UPS spectrum shifted toward lower binding energy, making the WF of the electrode 5.54 ± 0.04 eV, approximately 0.4 eV higher than bare gold. On the other hand, the **M9** SAM shifted the $E_{SC}$ of the electrode toward higher binding energy, making the effective WF of the modified surface 4.74 ± 0.04 eV, about 0.4 eV lower than bare gold. To modulate WF to intermediate values, **M1** and **M9** isomers were codeposited from the solutions of varying isomer ratios, that is, **M1**:**M9** = 3:1, 1:1, 1:3, and 1:5. Results indicated that each solution produces the effective gold WFs of 5.39 ± 0.03, 5.25 ± 0.03, 5.16 ± 0.02, and 5.01 ± 0.05 eV, respectively. As the molecular interactions of the isomers may differ from each other, the surface coverage ratios could be different from the solution concentration ratios.[39,44] To determine the surface coverage ratios of **M1** and **M9**, polarization modulation infrared reflection adsorption spectroscopy (PM-IRRAS) was performed and the obtained spectra were deconvoluted based on the individual spectrum of **M1** and **M9** (Figure S1, Supporting Information). Because of favorable dipole−dipole interactions between **M1** isomers, it was found that the surface coverage ratio of **M1** is typically higher than its solution proportions, as previously reported.[39] When the WFs of the SAM-modified electrodes were plotted against the surface coverage of **M1**, we found strong correlation to the isomer ratio present on the surface (Figure 1c). As the surface coverage of **M1** increases, the effective WF of gold increased approximately linearly. This suggests that, in principle, more precise tuning of gold WF can be achieved by carefully determining the relative concentrations of **M1** and **M9**. Although we cannot exclude the possibility of phase separation within the mixed SAMs, the sizes of phase-separated domains are usually on the nanometer scale[44−46] and should


dx.doi.org/10.1021/nl501081q | *Nano Lett.* 2014, 14, 2946−2951

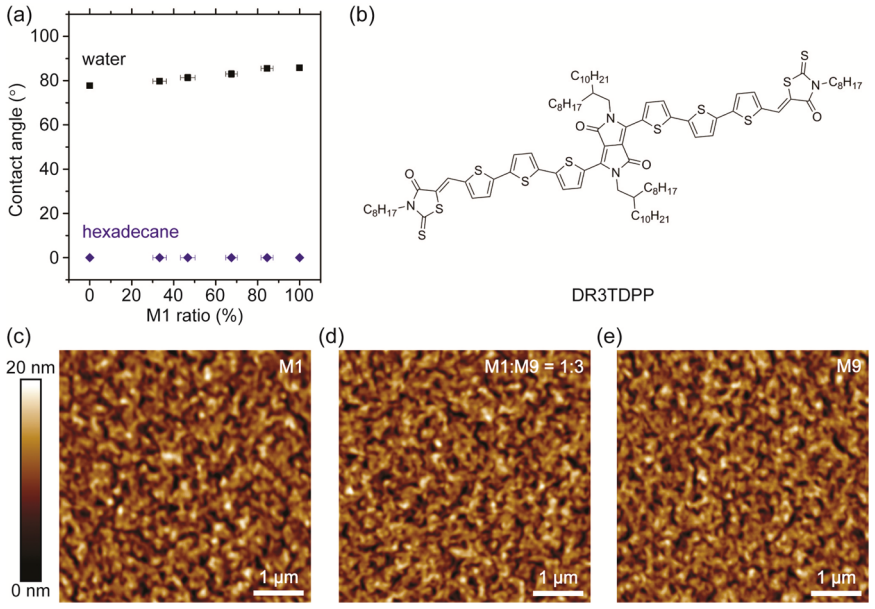


**Figure 2.** Minimal variation in surface wettability. (a) As the surface coverage of **M1** increases, the water contact angle gradually increases from 77.7° (100% **M9**) to 85.8° (100% **M1**) while hexadecane wets the surface completely in all cases, resulting in relatively small variations in surface energy. (b) Chemical structure of solution-processable organic semiconductor DR3TDPP. (c–e) AFM images of DR3TDPP thin films spin-coated on the gold surface modified with (c) **M1**, (d) **M1**:**M9** = 1:3, or (e) **M9**, respectively. No significant difference in the thin film morphology is observed.

not significantly affect macroscopic properties such as WF or surface wettability.

Next, we performed contact angle goniometry to determine the surface wettability of the SAM-modified gold surfaces (Figure 2a). We used water and hexadecane as probe liquids to measure the polar and dispersive component of solid surface energy, respectively. As the surface coverage of **M1** increases, the water contact angle gradually increased from 77.7 ± 0.8° (100% **M9**) to 85.8 ± 1.1° (100% **M1**). This small increase in the water contact angle could be attributed to the fact that **M1** has a smaller dipole moment compared to **M9**. The dispersive components of surface energies could not be differentiated among the mixed SAMs, however, as hexadecane wets the surface completely (contact angle = 0°), regardless of isomer ratios. In comparison, mixed SAMs consisting of alkanethiol and its fluorinated analogue show the hexadecane contact angle variations over 30°.[31] By applying the geometrical mean model developed by Owens and Wendt,[47] the total solid surface energies of the mixed SAMs were calculated to be 31.7 (**M1**), 31.8 (**M1**:**M9** = 3:1), 32.7 (**M1**:**M9** = 1:1), 33.4 (**M1**:**M9** = 1:3), 34.1 (**M1**:**M9** = 1:5), and 35.0 mN $m^{-1}$ (**M9**). Because the carboranethiol isomers are such similar molecules, the variation in the dispersive component of the surface energy should be minimal although the polar component varies as the ensemble of the surface dipole moments changes. Therefore, the surface energy variation among the mixed SAMs can be minimized (~3 mN $m^{-1}$), while the WF of the metal can be considerably modulated in both directions (~±0.4 eV). This is in stark contrast to other mixed SAM systems in which different chemical functionalities introduced to modify the metal WF inevitably induce significant variations in surface energies. Likewise, the symmetry of the upright, symmetric cage molecules leads to simply prepared, high-quality films, unlike linear molecules that have conformational relaxation and a plethora of defects in SAMs.[39,40,48] Therefore, the mixed SAMs of carboranethiol isomers can provide a robust platform for the fabrication and the study of solution-processed organic electronic devices in which the effect of the WF modulation can be independently monitored without interferences from other surface properties.

As the mixed SAMs of carboranethiol isomers share essentially identical chemical compositions with almost no difference in the surface energy, solution-processed organic layers deposited on top should possess similar thin film properties regardless of the isomer types or ratios used. To demonstrate this, we spin-coated a solution-processable semiconducting molecule 3,6-bis(5″-((*Z*)-(3-octyl-4-oxo-2-thioxothiazolidin-5-ylidene)methyl)-[2,2′:5′,2″-terthiophen]-5-yl)-2,5-bis(2-octyldodecyl)-2,5-dihydropyrrolo[3,4-*c*]pyrrole-1,4-dione (Figure 2b, DR3TDPP) onto SAM-modified gold substrates. We chose DR3TDPP (synthesis described in the Supporting Information) as our model organic semiconductor for its high solubility in various organic solvents and appropriate energy levels. Atomic force microscopy (AFM) images of the as-prepared DR3TDPP thin films on gold substrates modified with **M1**, **M1**:**M9** = 1:3 (surface coverage of **M1** near 50%), and **M9** are shown in Figure 2c–e, respectively. It was found that regardless of the surface isomer ratios, DR3TDPP formed grainy structures with similar grain sizes, and no significant difference in the thin film morphology could be observed. The root-mean-square roughnesses of the films were calculated to be within a narrow range, that is, 3.91, 3.94, and 3.48 nm for the **M1**, **M1**:**M9** = 1:3, or **M9**-modified surfaces, respectively. The thicknesses of the films were determined to be similar as well by profilometry, measuring approximately 70 nm for all cases. For even thinner DR3TDPP films with thickness of less than 10 nm, no significant difference in surface morphology could be observed under AFM (Figure S2, Supporting Information), suggesting that the thin film morphology at the interface is largely unaffected. Combining these results with the WF modulation confirmed by UPS measurements (Figure 1b), we conclude that the device performance variations among the DR3TDPP OFETs constructed with the carboranethiol SAM-modified electrodes can


dx.doi.org/10.1021/nl501081q | *Nano Lett.* 2014, 14, 2946–2951

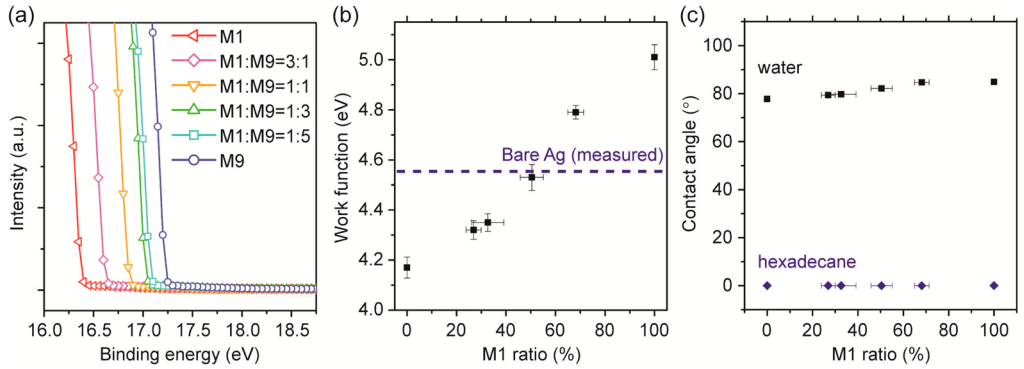


**Figure 3.** WF modulation of silver using mixed carboranethiol SAMs. As in the case of gold, (a) UPS measurements show that the WF of silver can be modulated by depositing the mixed SAMs of carboranethiol isomers with varying **M1**/**M9** ratios. As the surface coverage of **M1** increases, (b) the WF of silver increases from 4.16 eV (100% **M9**) to 5.01 eV (100% **M1**) with (c) minimal variations in water and hexadecane contact angles. The WF of bare silver was measured to be 4.56 eV (b, dashed line).

**Table 1. Summary of the Surface Properties of the Mixed Carboranethiol-SAM-Modified Gold and Silver**

| composition (in solution) | work function (Au) | contact angle (water, Au) | surface energy (Au) | work function (Ag) | contact angle (water, Ag) | surface energy (Ag) |
|---|---|---|---|---|---|---|
| M1 | 5.54 ± 0.04 eV | 85.8 ± 1.1° | 31.7 mN m$^{-1}$ | 5.01 ± 0.05 eV | 84.9 ± 0.9° | 32.0 mN m$^{-1}$ |
| M1:M9 = 3:1 | 5.39 ± 0.03 eV | 85.5 ± 0.8° | 31.8 mN m$^{-1}$ | 4.79 ± 0.03 eV | 84.7 ± 0.8° | 32.1 mN m$^{-1}$ |
| M1:M9 = 1:1 | 5.25 ± 0.03 eV | 83.0 ± 1.5° | 32.7 mN m$^{-1}$ | 4.53 ± 0.05 eV | 82.2 ± 0.8° | 33.0 mN m$^{-1}$ |
| M1:M9 = 1:3 | 5.16 ± 0.02 eV | 81.4 ± 1.5° | 33.4 mN m$^{-1}$ | 4.35 ± 0.03 eV | 79.7 ± 0.8° | 34.1 mN m$^{-1}$ |
| M1:M9 = 1:5 | 5.01 ± 0.05 eV | 79.7 ± 1.0° | 34.1 mN m$^{-1}$ | 4.32 ± 0.04 eV | 79.4 ± 0.8° | 34.3 mN m$^{-1}$ |
| M9 | 4.74 ± 0.04 eV | 77.7 ± 0.8° | 35.0 mN m$^{-1}$ | 4.16 ± 0.04 eV | 77.8 ± 1.0° | 35.0 mN m$^{-1}$ |

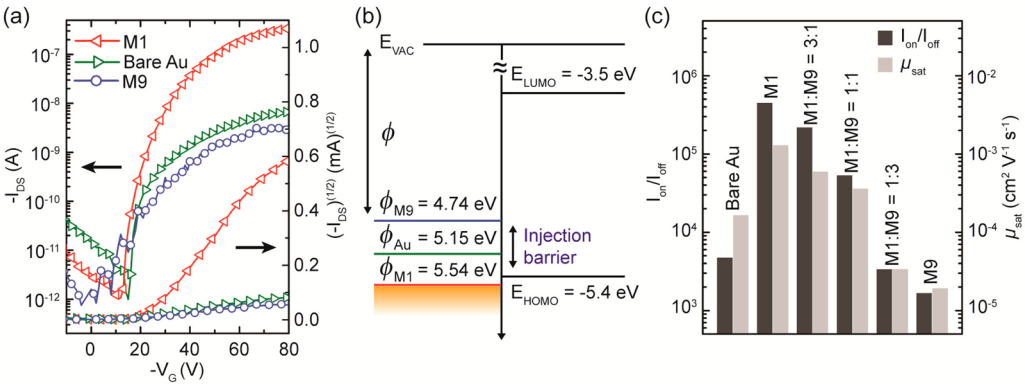


**Figure 4.** Charge injection modulation in solution-processed OFETs using the mixed SAMs. (a) Transfer characteristics ($V_D$ = −80 V) of DR3TDPP OFETs with different gold S/D electrodes. The **M1**-modified electrodes produce greatly enhanced device performance compared to bare or **M9**-modified electrodes. (b) Schematic energy level diagram of the gold electrodes and DR3TDPP. **M1** SAM increases the WF ($\phi$) of gold from 5.15 to 5.54 eV, lowering the hole injection barrier and thus enhances the charge injection. In contrast, **M9** SAM decreases the WF to 4.74 eV, resulting in larger hole injection barrier and poor device performance. As a result, (c) the on/off current ratio ($I_{on}/I_{off}$, dark gray) and the field-effect mobility ($\mu_{sat}$, light gray) of the OFETs decrease with increasing **M9** ratio.

be attributed to the change in the charge injection barrier height at the interface, as discussed below.

Carboranethiol isomers can form SAMs on other metals as well, such as silver[49] and copper,[50] and affect their WFs. We deposited mixed SAMs of varying **M1**/**M9** ratios on silver and repeated the surface characterizations performed on gold. Ag{111} substrates were prepared by electron-beam evaporation onto silicon wafers and used immediately without further treatment to minimize surface oxidation. Figure 3a shows UPS spectra collected from the modified silver surfaces. The WF of bare silver was measured to be 4.56 ± 0.04 eV (not shown). When the silver surface was decorated with an **M1** SAM, the $E_{SC}$ of the spectrum shifted toward lower binding energy, making the WF of the surface 5.01 ± 0.05 eV, about 0.45 eV higher than bare silver. In contrast, the **M9** SAM shifted the $E_{SC}$ toward higher binding energy, rendering the effective WF of the modified surface 4.16 ± 0.04 eV, about 0.4 eV lower than bare silver. The mixed SAMs deposited from the solutions of varying **M1**/**M9** ratios, that is, **M1**:**M9** = 3:1, 1:1, 1:3, and 1:5, resulted in the silver WFs of 4.79 ± 0.03, 4.53 ± 0.05, 4.35 ± 0.03, and 4.32 ± 0.04 eV, respectively. When the WFs of the SAM-modified silver surfaces were plotted against the surface coverage of **M1** deduced from the PM-IRRAS analysis (Figure S3, Supporting Information), we confirmed that there is a strong correlation between the WF and the isomer ratio present on the surface (Figure 3b) as in the case for gold. Contact angle goniometry measurements showed that there is only a slight increase in the water contact angle as the surface coverage of


dx.doi.org/10.1021/nl501081q | Nano Lett. 2014, 14, 2946−2951

**M1** increases while hexadecane wets the surface completely in all cases, suggesting that the WF of silver can also be modulated without significant changes in the surface energy. The WF, water contact angle, and surface energy of the modified gold and silver surfaces are summarized in Table 1.

On the basis of these results, we employed carboranethiol SAMs to study the charge injection process of the solution-processed DR3TDPP OFETs. Because the mixed SAMs can independently modulate the metal WF without causing significant variations in the thin film properties of the subsequent organic layers, the energy level alignment at the metal/semiconductor interface should account for the device performance modulation of the OFETs. We employed the bottom-gate/bottom-contact (BGBC) configuration using a heavily doped p-type silicon wafer covered with a thermally grown $SiO_2$ layer (200 nm). Gold S/D electrodes were deposited by electron-beam evaporation through a prepatterned mask and treated with **M1** and **M9** isomers of varying ratios to modulate the WF. After SAM deposition, the substrates were transferred into a $N_2$-filled glovebox, and a 1 wt % chloroform solution of DR3TDPP was spin-coated onto the substrates to complete devices. At least 40 devices were fabricated for each set of conditions, and the ten best devices were selected to calculate the average values of OFET parameters. Figure 4a shows the typical transfer characteristics of the as-fabricated OFETs (drain voltage, $V_D = -80$ V). The OFETs constructed with bare gold S/D electrodes showed well-behaved p-channel transistor performance with an on/off current ratio ($I_{on}/I_{off}$) of $(4.78 \pm 1.28) \times 10^3$ and a field-effect mobility ($\mu_{sat}$) of $(1.67 \pm 0.51) \times 10^{-4}$ cm$^2$ V$^{-1}$ s$^{-1}$ on average. With **M1**-modified gold electrodes, device performance was significantly enhanced with $I_{on}/I_{off}$ of $(4.53 \pm 1.19) \times 10^5$ and $\mu_{sat}$ of $(1.30 \pm 0.42) \times 10^{-3}$ cm$^2$ V$^{-1}$ s$^{-1}$ on average. In contrast, **M9** modification adversely affected device performance, resulting in $I_{on}/I_{off}$ of $(1.68 \pm 0.62) \times 10^3$ and $\mu_{sat}$ of $(1.94 \pm 0.58) \times 10^{-5}$ cm$^2$ V$^{-1}$ s$^{-1}$ on average. Compared to the OFETs constructed with the bare or **M1**-modified gold electrodes, the transfer characteristics of the **M9**-modified devices showed much higher noise levels, suggesting poor interfaces between the metal and the semiconductor. Figure 4b shows the schematic energy level diagram of the gold electrodes and DR3TDPP. The $E_{HOMO}$ and $E_{LUMO}$ of DR3TDPP were estimated to be −5.4 and −3.5 eV, respectively, by cyclic voltammetry (Figure S4, Supporting Information). Therefore, there is a considerable hole injection barrier (~0.25 eV) between the Fermi level of bare gold and $E_{HOMO}$ of DR3TDPP. This injection barrier can be greatly reduced by placing the **M1** SAM at the interface. In contrast, **M9** SAM further increases the injection barrier and thus leads to poor device performance. Figure 4c shows average values of $I_{on}/I_{off}$ and $\mu_{sat}$ of the OFETs constructed with the mixed SAMs of varying **M1**/**M9** ratios. Because the current injection at the metal/semiconductor interface can be described by the thermionic emission model,[1,6] a decrease in the injection barrier should result in an exponential increase in the on current, leading to greatly enhanced OFET performance. The enhanced current injection across the metal/semiconductor interface also leads to improvements in overall charge transport within the devices, resulting in higher $\mu_{sat}$.[51,52] As the surface coverage of **M9** increases, however, the WF should decrease, resulting in larger hole injection barriers and degradation in OFET performance. This trend was observed by comparing the OFETs with different surface modifications, demonstrating unambiguous correlation between the metal WF and the device performance.

We demonstrated that by using SAMs of carboranethiol isomers the WF of gold and silver can be systematically altered without causing a significant variation in surface energy. This independent control over the metal WF is made possible by the symmetric cage structures of carboranethiols, as they enable control of dipole moments without introducing additional chemical functionality. The symmetry of the compact and upright cage molecules leads to simply prepared, high-quality SAMs that have greatly reduced number of defects.[39−42] Continuous modulation of metal WF was achieved over a considerable range (~0.8 eV) with small changes in the surface energy (~3 mN m$^{-1}$) by codepositing two carboranethiol isomers with substantially different dipole directions. Therefore, mixed SAMs of carboranethiol isomers can provide an ideal platform to study the device physics of solution-processed OFETs where the performance variations caused by different surface energies can be minimized. We demonstrated that the injection barrier height at the metal/semiconductor interface can be modulated and efficient charge injection can be achieved by employing carboranethiol SAM-modified electrodes in solution-processed OFETs. With abundant functionalization chemistry readily available,[43] we anticipate that carboranes, related molecules, and their derivatives provide unique opportunities at the interfaces of chemistry, materials science, and nanoscience.

## ■ ASSOCIATED CONTENT

### Ⓢ Supporting Information

Materials and methods, synthesis of DR3TDPP, PM-IRRAS spectra of pure or mixed SAMs on gold and silver, AFM images of DR3TDPP thin films (<10 nm), and cyclic voltammogram of DR3TDPP. This material is available free of charge via the Internet at http://pubs.acs.org.

## ■ AUTHOR INFORMATION


### Corresponding Authors

*E-mail: yangy@ucla.edu (Y.Y.).
*E-mail: psw@cnsi.ucla.edu (P.S.W.).

### Author Contributions

‖J.K. and Y.S.R. contributed equally to this work.


### Notes

The authors declare no competing financial interest.

## ■ ACKNOWLEDGMENTS


This work is supported by the National Science Foundation through Grant CHE-1013042 and the Kavli Foundation. Y.S.R., Y.L., H.C., and Y.Y. acknowledge financial support from the National Science Foundation (DMR-1210893; Program manager: Dr. Andrew Lovinger). We thank the Nano and Pico Characterization Lab and the Integrated Systems Nanofabrication Cleanroom at the California NanoSystems Institute, and the UCLA Molecular Instrumentation Center for the use of their facilities.


## ■ REFERENCES


(1) Brütting, W.; Adachi, C.; Holmes, R. J. D. *Physics of Organic Semiconductors*, 2nd ed.; Wiley-VCH: Weinheim, 2012.
(2) Forrest, S. R. *Nature* **2004**, *428*, 911−918.
(3) Sirringhaus, H. *Adv. Mater.* **2014**, *26*, 1319−1335.
(4) Allard, S.; Forster, M.; Souharce, B.; Thiem, H.; Scherf, U. *Angew. Chem., Int. Ed.* **2008**, *47*, 4070−4098.

(5) Sirringhaus, H. *Adv. Mater.* **2005**, *17*, 2411−2425.
(6) Bao, Z.; Locklin, J. J. *Organic Field-Effect Transistors*; CRC Press: Boca Raton, FL, 2007.
(7) Cahen, D.; Kahn, A.; Umbach, E. *Mater. Today* **2005**, *8*, 32−41.
(8) Ma, H.; Yip, H. L.; Huang, F.; Jen, A. K. Y. *Adv. Funct. Mater.* **2010**, *20*, 1371−1388.
(9) Natali, D.; Caironi, M. *Adv. Mater.* **2012**, *24*, 1357−1387.
(10) Eom, S. H.; Baek, M.-J.; Park, H.; Yan, L.; Liu, S.; You, W.; Lee, S.-H. *ACS Appl. Mater. Interfaces* **2013**, *6*, 803−810.
(11) Bürgi, L.; Richards, T. J.; Friend, R. H.; Sirringhaus, H. *J. Appl. Phys.* **2003**, *94*, 6129−6137.
(12) Chua, L. L.; Zaumseil, J.; Chang, J. F.; Ou, E. C. W.; Ho, P. K. H.; Sirringhaus, H.; Friend, R. H. *Nature* **2005**, *434*, 194−199.
(13) Wang, S. D.; Minari, T.; Miyadera, T.; Tsukagoshi, K.; Aoyagi, Y. *Appl. Phys. Lett.* **2007**, *91*, 203508.
(14) Chu, C.-W.; Li, S.-H.; Chen, C.-W.; Shrotriya, V.; Yang, Y. *Appl. Phys. Lett.* **2005**, *87*, 193508.
(15) Kumaki, D.; Umeda, T.; Tokito, S. *Appl. Phys. Lett.* **2008**, *92*, 013301.
(16) Li, S.-H.; Xu, Z.; Yang, G.; Ma, L.; Yang, Y. *Appl. Phys. Lett.* **2008**, *93*, 213301.
(17) Zhou, Y.; Fuentes-Hernandez, C.; Shim, J.; Meyer, J.; Giordano, A. J.; Li, H.; Winget, P.; Papadopoulos, T.; Cheun, H.; Kim, J.; Fenoll, M.; Dindar, A.; Haske, W.; Najafabadi, E.; Khan, T. M.; Sojoudi, H.; Barlow, S.; Graham, S.; Brédas, J.-L.; Marder, S. R.; Kahn, A.; Kippelen, B. *Science* **2012**, *336*, 327−332.
(18) Helander, M. G. *Science* **2012**, *336*, 302−303.
(19) Campbell, I. H.; Rubin, S.; Zawodzinski, T. A.; Kress, J. D.; Martin, R. L.; Smith, D. L.; Barashkov, N. N.; Ferraris, J. P. *Phys. Rev. B* **1996**, *54*, R14321−R14324.
(20) Hamadani, B. H.; Corley, D. A.; Ciszek, J. W.; Tour, J. M.; Natelson, D. *Nano Lett.* **2006**, *6*, 1303−1306.
(21) Marmont, P.; Battaglini, N.; Lang, P.; Horowitz, G.; Hwang, J.; Kahn, A.; Amato, C.; Calas, P. *Org. Electron.* **2008**, *9*, 419−424.
(22) Cheng, X. Y.; Noh, Y. Y.; Wang, J. P.; Tello, M.; Frisch, J.; Blum, R. P.; Vollmer, A.; Rabe, J. P.; Koch, N.; Sirringhaus, H. *Adv. Funct. Mater.* **2009**, *19*, 2407−2415.
(23) DiBenedetto, S. A.; Facchetti, A.; Ratner, M. A.; Marks, T. J. *Adv. Mater.* **2009**, *21*, 1407−1433.
(24) Boudinet, D.; Benwadih, M.; Qi, Y. B.; Altazin, S.; Verilhac, J. M.; Kroger, M.; Serbutoviez, C.; Gwoziecki, R.; Coppard, R.; Le Blevennec, G.; Kahn, A.; Horowitz, G. *Org. Electron.* **2010**, *11*, 227−237.
(25) Kim, S. H.; Lee, S. H.; Jang, J. *IEEE Electron Device Lett.* **2010**, *31*, 1044−1046.
(26) Bauert, T.; Zoppi, L.; Koller, G.; Garcia, A.; Baldridge, K. K.; Ernst, K.-H. *J. Phys. Chem. Lett.* **2011**, *2*, 2805−2809.
(27) Lenz, T.; Schmaltz, T.; Novak, M.; Halik, M. *Langmuir* **2012**, *28*, 13900−13904.
(28) Claridge, S. A.; Liao, W. S.; Thomas, J. C.; Zhao, Y. X.; Cao, H. H.; Cheunkar, S.; Serino, A. C.; Andrews, A. M.; Weiss, P. S. *Chem. Soc. Rev.* **2013**, *42*, 2725−2745.
(29) Alloway, D. M.; Hofmann, M.; Smith, D. L.; Gruhn, N. E.; Graham, A. L.; Colorado, R.; Wysocki, V. H.; Lee, T. R.; Lee, P. A.; Armstrong, N. R. *J. Phys. Chem. B* **2003**, *107*, 11690−11699.
(30) Heimel, G.; Romaner, L.; Zojer, E.; Bredas, J.-L. *Acc. Chem. Res.* **2008**, *41*, 721−729.
(31) Wu, K. Y.; Yu, S. Y.; Tao, Y. T. *Langmuir* **2009**, *25*, 6232−6238.
(32) Chen, C. Y.; Wu, K. Y.; Chao, Y. C.; Zan, H. W.; Meng, H. F.; Tao, Y. T. *Org. Electron.* **2011**, *12*, 148−153.
(33) Kim, D. H.; Jang, Y.; Park, Y. D.; Cho, K. *Langmuir* **2005**, *21*, 3203−3206.
(34) Asadi, K.; Gholamrezaie, F.; Smits, E. C. P.; Blom, P. W. M.; de Boer, B. *J. Mater. Chem.* **2007**, *17*, 1947−1953.
(35) Love, J. C.; Estroff, L. A.; Kriebel, J. K.; Nuzzo, R. G.; Whitesides, G. M. *Chem. Rev.* **2005**, *105*, 1103−1170.
(36) Poirier, G. E. *Chem. Rev.* **1997**, *97*, 1117−1128.
(37) Weiss, P. S. *Acc. Chem. Res.* **2008**, *41*, 1772−1781.
(38) Base, T.; Bastl, Z.; Plzak, Z.; Grygar, T.; Plesek, J.; Carr, M. J.; Malina, V.; Subrt, J.; Bohacek, J.; Vecernikova, E.; Kriz, O. *Langmuir* **2005**, *21*, 7776−7785.
(39) Hohman, J. N.; Zhang, P. P.; Morin, E. I.; Han, P.; Kim, M.; Kurland, A. R.; McClanahan, P. D.; Balema, V. P.; Weiss, P. S. *ACS Nano* **2009**, *3*, 527−536.
(40) Hohman, J. N.; Claridge, S. A.; Kim, M.; Weiss, P. S. *Mater. Sci. Eng., R* **2010**, *70*, 188−208.
(41) Kim, M.; Hohman, J. N.; Morin, E. I.; Daniel, T. A.; Weiss, P. S. *J. Phys. Chem. A* **2009**, *113*, 3895−3903.
(42) Hohman, J. N.; Kim, M.; Schüpbach, B.; Kind, M.; Thomas, J. C.; Terfort, A.; Weiss, P. S. *J. Am. Chem. Soc.* **2011**, *133*, 19422−19431.
(43) Grimes, R. N. *Carboranes*, 2nd ed.; Academic Press: Burlington, MA, 2011.
(44) Smith, R. K.; Reed, S. M.; Lewis, P. A.; Monnell, J. D.; Clegg, R. S.; Kelly, K. F.; Bumm, L. A.; Hutchison, J. E.; Weiss, P. S. *J. Phys. Chem. B* **2001**, *105*, 1119−1122.
(45) Stranick, S. J.; Parikh, A. N.; Tao, Y. T.; Allara, D. L.; Weiss, P. S. *J. Phys. Chem.* **1994**, *98*, 7636−7646.
(46) Stranick, S. J.; Atre, S. V.; Parikh, A. N.; Wood, M. C.; Allara, D. L.; Winograd, N.; Weiss, P. S. *Nanotechnology* **1996**, *7*, 438−442.
(47) Owens, D. K.; Wendt, R. C. *J. Appl. Polym. Sci.* **1969**, *13*, 1741−1747.
(48) Saavedra, H. M.; Mullen, T. J.; Zhang, P.; Dewey, D. C.; Claridge, S. A.; Weiss, P. S. *Rep. Prog. Phys.* **2010**, *73*, 036501.
(49) Base, T.; Bastl, Z.; Havranek, V.; Lang, K.; Bould, J.; Londesborough, M. G. S.; Machacek, J.; Plesek, J. *Surf. Coat. Technol.* **2010**, *204*, 2639−2646.
(50) Base, T.; Bastl, Z.; Havranek, V.; Machacek, J.; Langecker, J.; Malina, V. *Langmuir* **2012**, *28*, 12518−12526.
(51) Ohta, T.; Nagano, T.; Ochi, K.; Kubozono, Y.; Shikoh, E.; Fujiwara, A. *Appl. Phys. Lett.* **2006**, *89*, 053508.
(52) Dong, H.; Fu, X.; Liu, J.; Wang, Z.; Hu, W. *Adv. Mater.* **2013**, *25*, 6158−6183.